Table 1. Composition of the feedstock (wt. %).

PX	MX	OX	EB	C_3	C_4	C_5	C_6^{N+P}	C_7^{N+P}	C_8^{N+P}	C_9^{A+n}	C_{10}^{A+n}	C_{11}+H	T	B
3.282	51.452	24.151	12.004	0.006	0.006	0.021	0.193	0.507	5.967	1.417	0.040	0.073	0.881	0.00

Notes: PX: p-xylene, MX: m-xylene, OX: o-xylene, EB: ethylbenzene, C_6^{N+P}: C_6 naphthenes and paraffin, C_7^{N+P}: C_7 naphthenes and paraffin, C_8^{N+P}: C_8 naphthenes and paraffin, C_9^{A+n}: C_9 Aromatic and nonaromatic, C_{10}^{A+n}: C_{10} Aromatic and nonaromatic, H: hydrocarbons, T: toluene, B: benzene.

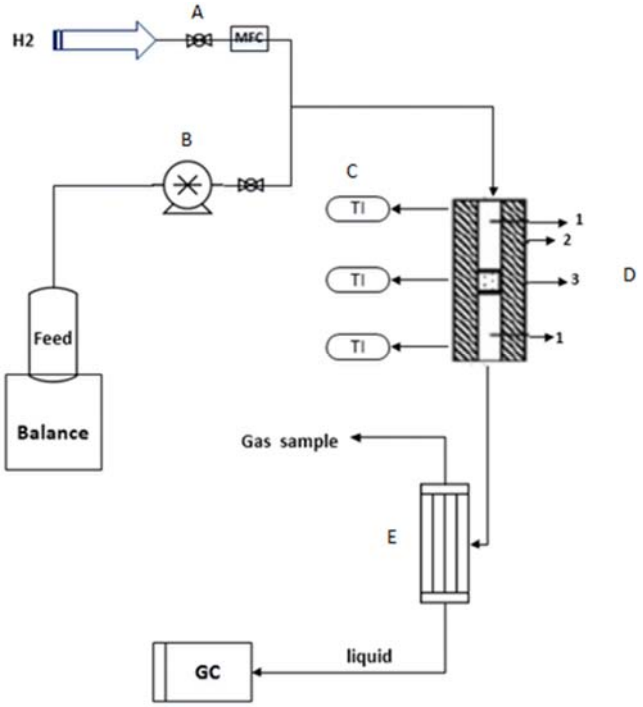

Fig. 2. The catalytic setup of m-xylene isomerization reaction (A) ball value, (B) HPLC pump, (C) temperature indicator, (D) isothermal reactor, (E) condenser, (1) quartz, (2) wool, (3) catalyst.

m-xylene conversion, p-xylene/o-xylene ratio and xylene loss were calculated according to the following equations:

MX conversion (%) = [(mass fraction of MX in a feedstock – mass fraction of MX in products) ÷ mass fraction of MX in feedstock] × 100 (1)

PX/OX (%) = (mass fraction of PX in products ÷ mass fraction of OX in products) × 100 (2)

Xylene loss (%) = {[mass fraction of (OX + MX + PX) in a feedstock – mass fraction of (OX + MX + PX) in products] ÷ mass fraction of (OX + MX + PX) in feedstock} × 100 (3)

(Mass fraction is based on wt. %)

3. Results and Discussion

3.1. FT-IR studies

Mordenite can be characterized by its infrared spectrum. FT-IR spectra of Na-mordenite sample is shown in Fig. 3. It has some main absorption regions, the peak around to 1083 cm^{-1} ascribed to the asymmetric stretching vibration of Si-O bond and another peak near to 810 cm^{-1} referring to symmetric stretching vibration of Al-O bond.

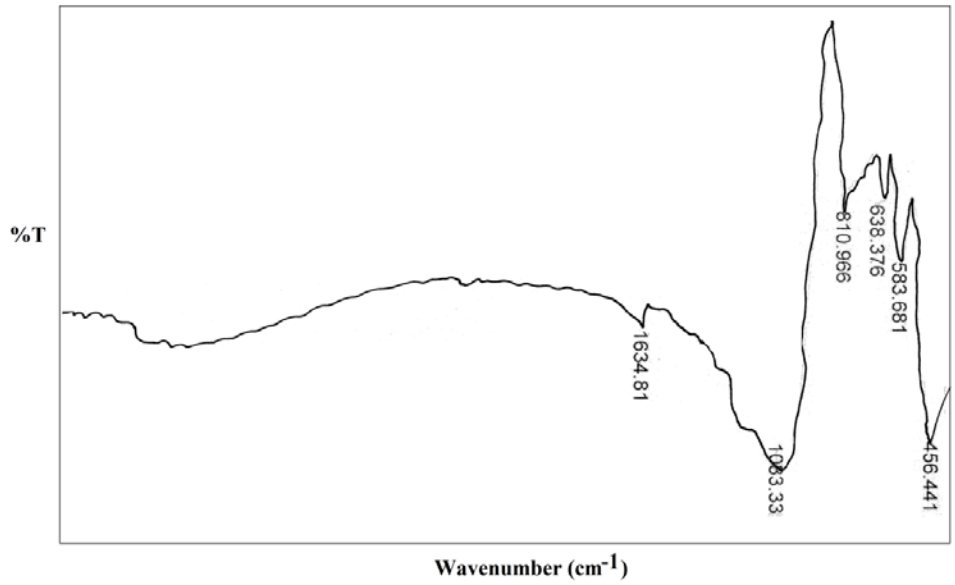

Fig. 3. FT-IR spectrum the prepared sample.

It also has a peak at 638 cm^{-1} belonged to SiO_4 and AlO_4 tetrahedral and a peak centered at 583 cm^{-1} related to the vibration of five-membered rings. The located peak at 456 cm^{-1} corresponding to bending vibration of T-O bond [12,13]. As shown in the previous references [13,22-24], all zeolitic vibration modes are present at the spectra of raw and H-form of sample, confirming that there was no significant difference between Na-mordenite and protonated form (H-form not shown).

3.2. X-ray diffraction studies

Fig. 4 shows the X-ray pattern of synthesized Na-mordenite. The strong diffraction peaks located at 2θ values range of 9° to 36° in the pattern, correspond to the reflections of mordenite structure [25]. The reflection peaks at 2θ values of 9.77°, 13.45°, 19.61°, 22.20°, 23.16°, 25.63°, 26.25°, 27.67°, 27.87°, 30.89° and 35.61° in XRD pattern of prepared zeolite were in agreement with the literature [13,19,25] and crystalline phases were identified using the Joint Committee on Powder Diffraction Standards (JCPDS) files (29-1257 corresponds to mordenite). This indicated that a highly crystalline and pure sample was formed. The XRD pattern of the H-form zeolites is essentially identical to those of the corresponding Na-form zeolites [26].

3.3. Surface area and SEM studies

The obtained data of prepared mordenite sample such as Si/Al ratio, surface area and pore volume are listed in Table 2. The BET results indicate that the synthesized mordenite has a large surface area.

The morphological characters of the synthesized mordenite were obtained by SEM. As shown in Fig. 5, the morphology and size of the synthesized mordenite is similar with other studies as reported already [13,19,27]. The average size of the sample was estimated about 5-7 μm.

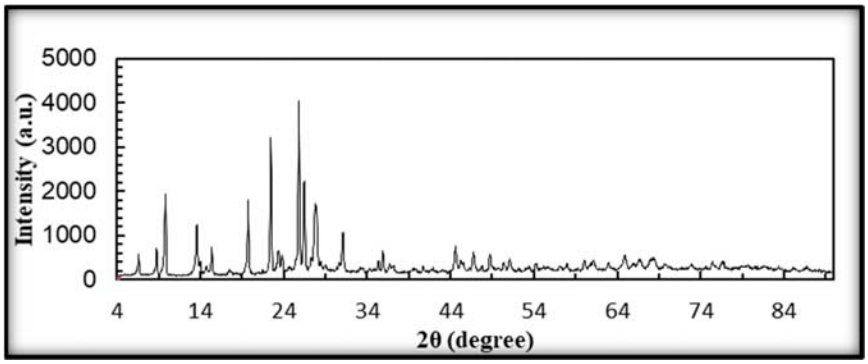

Fig. 4. XRD pattern of mordenite.

Table 2. Properties of mordenite.

Unit cell parameters (Å)			Si/Al ratio	BET surface area (m^2g^{-1})	Pore volume (m^3g^{-1})
a	b	c			
18.1	20.5	7.5	18	331.63	0.278

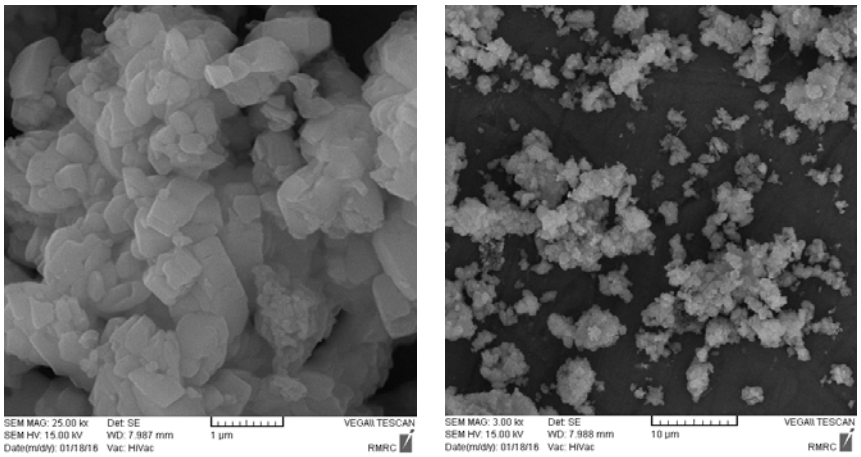

Fig. 5. SEM images of mordenite.

3.4. Catalytic application of synthesized mordenite

In order to investigate the application of the prepared zeolite in m-xylene isomerization reaction, the synthesized mordenite sample was tested in a fixed bed catalytic setup and the results were compared with a commercial SAPO-11 catalyst (Si/Al = 20) provided by Zeolyst International. The results of meta-xylene conversion to para-xylene on two zeolites are shown in Table 3 at pressure of 10 bars and temperature of 380°C in 2 reaction times: 6h and 12h.

According to the results depicted in Table 3, over two catalysts, when the time of reaction increased from 6h to 12h, the amount of para-xylene which was produced was decreased whereas, the amounts of meta-xylene which was produced and xylene loss were increased.

Table 3. Comparison of catalytic activity of prepared mordenite catalyst with commercial SAPO-11 catalyst in m-xylene isomerization reaction.

Catalyst	Mordenite		SAPO-11	
Temp. (°C)	380	380	380	380
Catalyst (g)	4	4	4	4
WHSV (1 h^{-1})	3.35	3.35	3.35	3.35
TOS (h)	6	12	6	12
p-xylene	13.20	10.96	10.07	8.81
m-xylene	43.78	43.97	43.01	44.19
o-xylene	20.74	21.16	21.05	21.81
ethylbenzene	6.63	8.40	9.86	10.35
C_3	0.01	0.01	0.01	0.01
C_4	0.05	0.04	0.06	0.06
C_5	0.26	0.12	0.19	0.15
C_6^P	0.24	0.10	0.14	0.14
C_6^N	0.36	0.24	0.08	0.05
C_7^P	0.25	0.03	0.04	0.06
C_7^N	0.29	0.31	0.43	0.35
C_8^P	2.02	2.53	3.19	3.11
C_8^N	4.39	6.30	7.09	6.12
C_9^n	2.58	3.18	2.67	3.26
C_9^A	2.11	0.08	0.17	0.05
C_{10}^n	0.00	0.00	0.02	0.00
C_{10}^A	0.106	0.076	0.092	0.020
C_{11} + H	0.10	0.08	0.21	0.07
Toluene	1.96	1.42	1.46	1.31
Benzene	0.92	0.55	0.12	0.09
MX conversion (%)	14.91	14.54	16.40	14.11
PX/OX (%)	63	52	48	40
Xylene loss (%)	2.11	3.54	6.03	5.16

*Note: TOS is Time-on-stream, The compositions are in wt.%.

3.5. Investigation of reaction time on m-xylene conversion over the zeolite catalysts

Conversion of m-xylene over zeolite catalysts is plotted against reaction time in Fig. 6. After the reaction time of 6 hours over mordenite, m-xylene conversion reached to 14.91% compared to 16.40% over SAPO-11. After the reaction time of 12 h, Fig. 6 shows that m-xylene conversion reached to 14.54% compared to 14.11% over the SAPO-11. It can be explained that acidic properties of SAPO-11 which is medium, increased in high temperature (>300°C) and therefore it be suitable for isomerization reaction [28].

According to the Fig. 6, when the reaction time increased from 6h to 12h, m-xylene conversion over two catalysts decreased.

3.6. Investigation of p-Xylene to o-xylene (P/O) ratio over the zeolite catalysts

The para to ortho ratio over mordenite and SAPO-11 are presented in Fig. 7 at both reaction times of 6 and 12h. As shown in Fig. 7, mordenite has a (P/O) ratio of 63% at 6 h that is greater than the SAPO-11 at 6 h (48%) and decrease to 52% at 12 h reaction time over mordenite and to 40% over SAPO-11. The higher P/O ratio over mordenite catalyst is due to the higher diffusivity of p-xylene into the large pore of mordenite compared to the medium pore of SAPO-11 (4 Å × 6.5 Å). p-Xylene quickly diffusion into the mordenite zeolite as soon it forms [29,30]. As can be seen in Fig. 7, with increasing the reaction time over both catalysts, the P/O ratio decreased.

Generally, the best time of this reaction for both catalysts at 380°C was 6h, because the amount of para-xylene which was produced, meta-xylene conversion and PX/OX ratio were higher but the amounts of meta-xylene which was produced and xylene loss were lower compared to 12h reaction time.

4. Conclusions

In this study, the mordenite zeolite was synthesized with high crystallinity in absence of templating agent. The performance of prepared zeolite in meta-xylene isomerization reaction in a fixed bed reactor was investigated and compared with the commercial SAPO-11 catalyst. Based on the results which were obtained from this study, our synthesized catalyst demonstrated higher para/ortho ratio, while keeping the loss of xylene lower compared to SAPO-11. These results are shown that totally, the prepared mordenite is a better catalyst than SAPO-11 in m-xylene isomerization reaction.

References

[1] G. Horacio, R. Abante, C. Luis, R. Jorge, Ind. Eng. Chem. Res. 35 (1996) 3964-3972.
[2] V. Sreedharan, S. Bhatia, J. Chem. Eng. 36 (1987) 101-109.
[3] P.K. Sen Sarma, S. Bhatia, Zeolites 7 (1987) 511-516.
[4] K. Ahmed, M. Sameh, A. Eman, M. Sahar, J. Chin. Chem. Soc. 51 (2004) 817-826.
[5] A. Nezamzadeh-Ejhieh, M. Khorsandi, Desalination 262 (2010) 79–85.
[6] D.G. Maia, C. Yolanda, S. Pilar, Microporous Mesoporous Mater. 144 (2011) 162-170.
[7] Sh. Aghabeygi, R. Kia Kojoori, H. Vakili Azad, Iran. J. Catal. 6 (2016) 275-279.
[8] A. Nezamzadeh-Ejhieh, Z. Salimi, Desalination 280 (2011) 281–287.
[9] M.H. Sheikh-Mohseni, A. Nezamzadeh-Ejhieh, Electrochim. Acta 147 (2014) 572–581.
[10] N. Samadani Langeroodi, Iran. J. Catal. 3 (2013) 79-82.
[11] A. Bagheri Ghomi, V. Ashayeri, Iran. J. Catal. 2 (2012) 135-140.
[12] M. Mohamed, M. Tarek, O. Ibraheem, A. Ibraheem, Microporous Mesoporous Mater. 84 (2005) 84-96.
[13] M. Hisham, E. Moustafa, A. Ehab, Powder Technol. 23 (2012) 757-760.

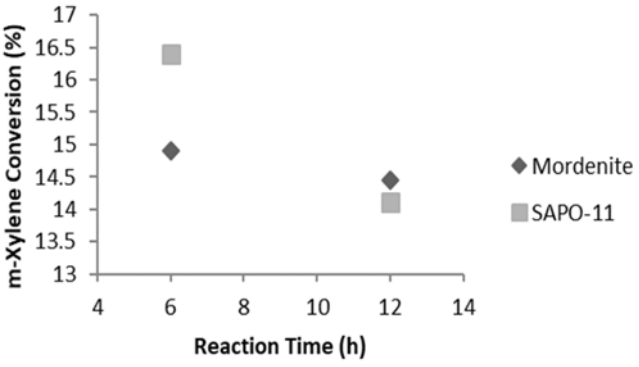

Fig. 6. m-Xylene conversions versus reaction time at 380°C over two catalysts.

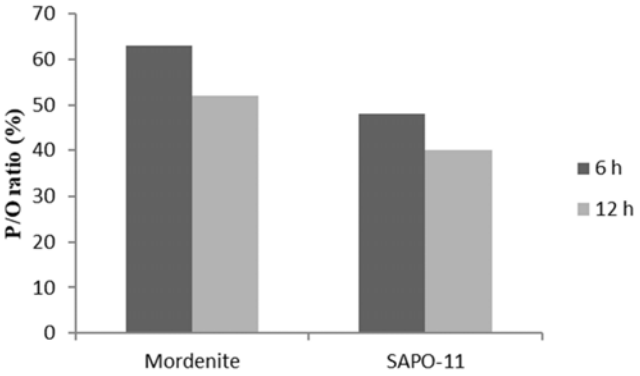

Fig. 7. P/O ratio over two catalysts at 6h and 12h reaction time.

[14] L. Xianfeng, P. Roel, A. Jeroen, J. Catal. 262 (2009) 257-265.
[15] T.C. Tsai, S.B. Liu, I. Wang, Appl. Catal. A 181 (1999) 355-398.
[16] C.H. Baerlocher, L.B. McCusker, D.H. Olson, Atlas of zeolite framework types, 6th Ed., Elsevier, USA, 2007.
[17] K.B. Pramod, M.S. Rao, K.V.G.K. Gokhale, Ind. Eng. Chem. Prod. Res. Dev. 17 (1978) 223-227.
[18] V. Nagabhatla, K. Manoj, Microporous Mesoporous Mater. 92 (2006) 31-37.
[19] L. MarceIo, I. Diego, R.C. Nádia, M. Fernandes, B.C. Sibele, Appl. Clay Sci. 41 (2008) 99-104.
[20] R. Xu, W. Pang, J. Yu, Q. Huo, J. Chen, Chemistry of zeolites and related porous materials, Wiley, Asia, 2007.
[21] G. Peng, L. Xiaofeng, Z. Shang, X. Qinghu, D. Tao, J. Pet. Sci. Eng. 9 (2012) 544-550.
[22] J. Bhadauriaa, B.K. Singhb, A. Tomarar, R. Tomara, J. Chem. Pharm. Res. 3 (2011) 245-257.
[23] J.C. Moreno-Piraján, V. S. Garcia-Cuello, L. Giraldo, J. Thermodyn. Catal. 1 (2010) 1-8.
[24] A. Nezamzadeh-Ejhieh, A. Shirzadi, Chemosphere 107 (2014) 136–144.
[25] M.M.J. Treacy, J.B. Higgins, Collection of simulated XRD powder patterns for zeolites, 4th Ed., Elsevier, Oxford, 2001.
[26] W. Yi, K. Yuichi, O. Toshio, Water Res. 41 (2007) 269-276.
[27] T. Selvam, W. Schwieger, Stud. Surf. Sci. Catal. 142 (2002) 407-414.
[28] Y. Liu, A. Yan, Q. Xu, Appl. Catal. A 67 (1991) 169-177.
[29] M. Filipa Ribeiro, F. Ramoa Ribeiro, P. Dufresne, C. Marcilly, J. Mol. Catal. 39 (1987) 269-276.
[30] N.M. Tukur, Al-K. S. Al-Khattaf, Chem. Eng. J. 166 (2011) 348-357.